Electronic Supplementary Material (ESI) for Nanoscale.
This journal is © The Royal Society of Chemistry 2023

Electronic Supplementary Material (ESI) for Nanoscale.
This journal is © The Royal Society of Chemistry 2022

BSA-templated synthesis of Ir/Gd bimetallic oxide nanotheranostics for MR/CT imaging-guided photothermal and photodynamic synergistic therapy

Chao Cai,[a#] Feng Tian,[b#] Junping Ma,[a] Zipei Yu,[a] Mo Yang [b] and Changqing Yi [a*]

[a]Guangdong Provincial Engineering and Technology Center of Advanced and Portable Medical Devices, School of Biomedical Engineering, Sun Yat-Sen University, Shenzhen 518107, China.

[b] Department of Biomedical Engineering, The Hong Kong Polytechnic University, Hong Kong, China

□ Equal contribution

Experimental

Photothermal effect of BSA@Gd_2O_3/IrO_2 NPs: 1 mL of BSA@Gd_2O_3/IrO_2 NPs aqueous solution with different Ir concentrations (0, 0.5, 1.0, 3.0, 6.0 mM) was added into a quartz and exposed to an 808 nm laser (1.5 W cm^{-2}) for 10 min. An ultra-sensitive thermometer is used to record the temperature change every 15 seconds. To evaluate the thermal stability of BSA@Gd_2O_3/IrO_2 NPs, 1 mL BSA@Gd_2O_3/IrO_2 NPs (6 mM: respect to Ir) aqueous solution was irradiated with an 808 nm laser (1.5 W cm^{-2}) for 10 min, the temperature is cooled to room temperature in the natural environment. Repeat the above process five times and record the temperature with a sensitive thermometer every 15 seconds.

The photothermal conversion efficiency (η) is calculated by the following equations.[1]

$$\theta = \left(T - T_{surr}\right) \div \left(T_{max} - T_{surr}\right) \quad (1)$$

$$t = \tau_s \times \left(- In\theta\right) \quad (2)$$

$$hS = \left(\sum m_i \, C_{p,i}\right) \div \tau_s \quad (3)$$

$$Q_{Dis} = hS \times \left(T\left(H_2O\right)_{max} - T_{surr}\right) \quad (4)$$

$$\eta = \left[hS \times \left(T_{max} - T_{surr}\right) - Q_{Dis}\right] \div \left[I \times \left(1 - 10^{-A808}\right)\right] \times 100\% \quad (5)$$

h (mW m^{-2} °C^{-1}): Heat transfer coefficient;

S (m^2): Surface area of container;

T_{max} (°C): Equilibrium temperature during laser irradiation;

T_{surr} (°C): Ambient temperature of the surrounding;

Q_{Dis} (mW): The heat from light absorbed by the quartz cuvette walls itself and was measured independently using a quarte cuvette containing aqueous solution without BSA@Gd_2O_3/IrO_2 NPs;

I: The irradiated laser power density;

A_{808}: The absorbance of BSA@Gd_2O_3/IrO_2 NPs (6 mM with respect to Ir) at 808 nm.

Biocompatibility: The cytotoxicity of BSA@Gd_2O_3/IrO_2 NPs was evaluated against HepG2, 4T1 and L02 cells using a standard MTT assay. In brief, the cells were cultured in 96-well plates at a density of 3×10^3 cells per well and allowed to adhere overnight. Then the cells were treated with BSA@Gd_2O_3/IrO_2 NPs at various concentrations (0, 0.25, 0.5, 1, 2, 4, 6, 8, 10 mM with respect to Ir) for 24h, the cell viabilities were measured by MTT assay.

The hemolytic test was performed using mouse blood cells. 0.5 mL BSA@Gd_2O_3/IrO_2 NPs with different concentrations (0, 50, 100, 150, 200, 250, 300, 350, 400 μg mL^{-1}) for 2 h at room temperature under mild shake. The samples were centrifuged at 1000 rpm for 10 min, and then, the upper supernatant was collected for measuring its absorbance at 541 nm to calculate the hemolysis rate by the following equation:

$$Hemolysis(\%) = \frac{A - A_{PBS}}{A_{TritonX-100} - A_{PBS}} \times 100\%$$

In the hemolysis assay, 0.5 mL of PBS and Triton-X 100 were used as negative and positive control, respectively. Besides, the sediments were re-dissolved in PBS for erythrocyte morphology observation.

Tumor models: All animal experiments were operated on the basis of national guidelines and approved by the Animal Experimentation Ethics Committee of Sun Yat-Sen University for animal treatment. To establish 4T1 tumor-bearing mice models, 100 μL of 4T1 cell suspension (1×10^7 cells mL^{-1}) were subcutaneously injected in the right

back of Balb/c mice (4-5 weeks, 15-20 g) and the tumors were allowed to grow to a uniform size around 150-200 mm^3.

Histology and HIF-1α staining: After different treatments, the mice were sacrificed and the tumor tissues, heart, Liver, spleen, lung and kidney were dissected from mice in different treatment schemes and fixed in 4% paraformaldehyde and processed routinely into paraffin. Then, the tumors and normal organs were sliced to 4 μm thickness for hematoxylin and eosin (H&E), TUNEL and HIF-1α staining, and the slices were observed by a digital microscope.

Blood routine and blood biochemical tests: On the 24^{th} day, the tumor-bearing mice in above treatment schemes were collected and their blood was drawn from the eye socket. The blood biochemical indexes of normal mice were set as control. The levels of alanine transaminase (ALT), alkaline phosphatase (ALP), creatinine (CREA), Albumin (ALB), Aspartate aminotransferase (AST), Urea nitrogen (BUN) and total protein (TP) were measured.

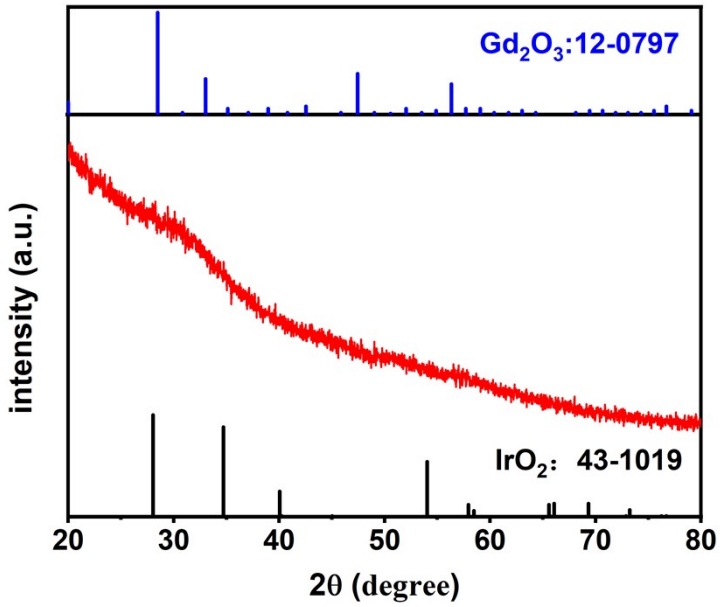

Figure S1. The X-ray diffraction pattern of BSA@Gd_2O_3/IrO_2 NPs.

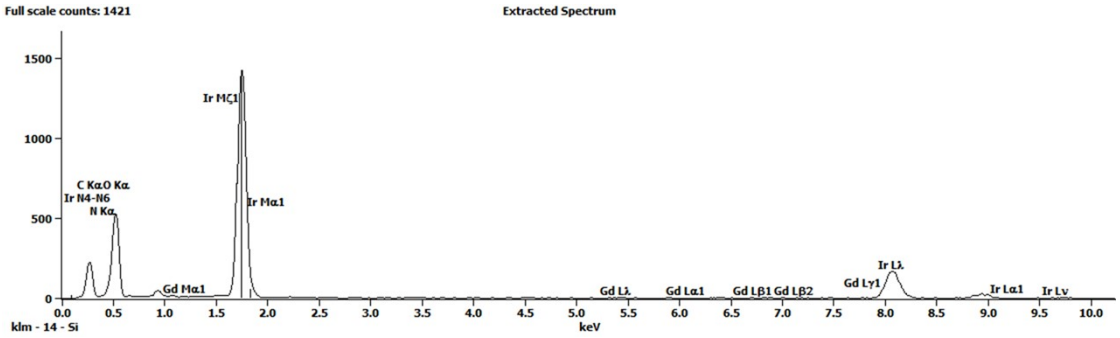

Figure S2. The EDS analysis of BSA@Gd_2O_3/IrO_2 NPs.

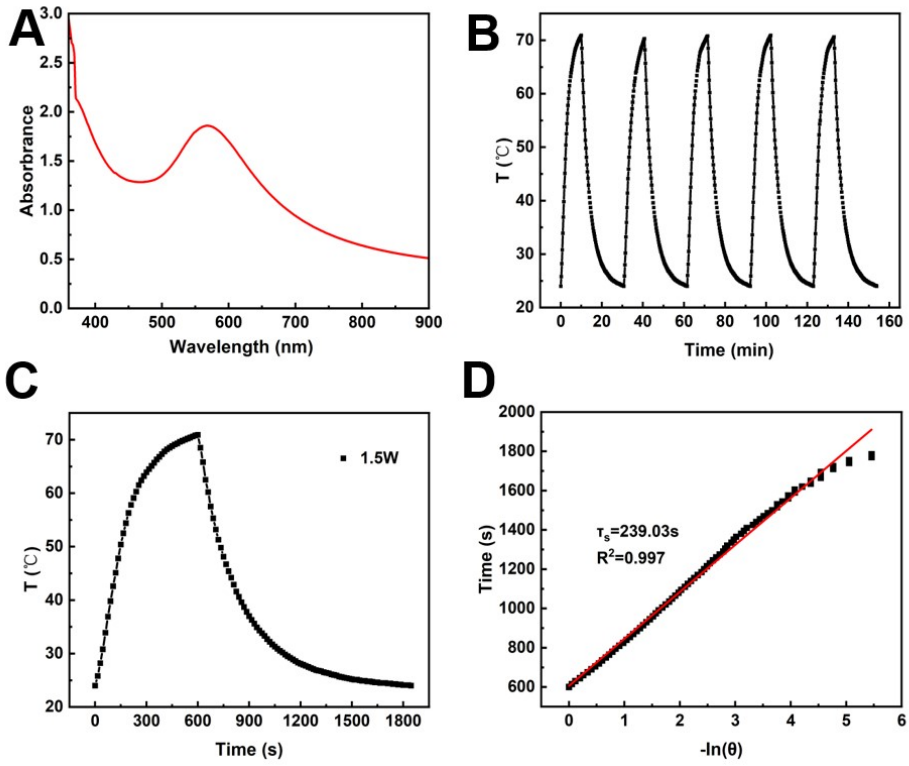

Figure S3. (A) UV-vis absorption spectrum of BSA@Gd_2O_3/IrO_2 NPs in aqueous solution; (B) Temperature records of BSA@Gd_2O_3/IrO_2 NPs aqueous solution (Ir equivalent concentration: 6 mM) under five cycles of laser on/off; (C) Photothermal effect of BSA@Gd_2O_3/IrO_2 NPs aqueous solution (Ir equivalent concentration: 6 mM) under irradiation of an 808 laser and the laser was turned off after irradiation for 10 min. (D) The time constant for heat transfer from the system was determined to be τ_s = 239.03 s by applying the linear time data from the cooling period (after 10 min) versus negative natural logarithm of the driving force temperature obtained from the cooling stage of (C).

Figure S4. Gas bubbles observed after incubation of 1.0 mM H_2O_2 with phosphate buffered solution (0.1 M, pH = 6.2) (Left) and BSA@Gd_2O_3/IrO_2 NPs (Ir equivalent concentration: 2.0 mM) (Right) for 5 min.

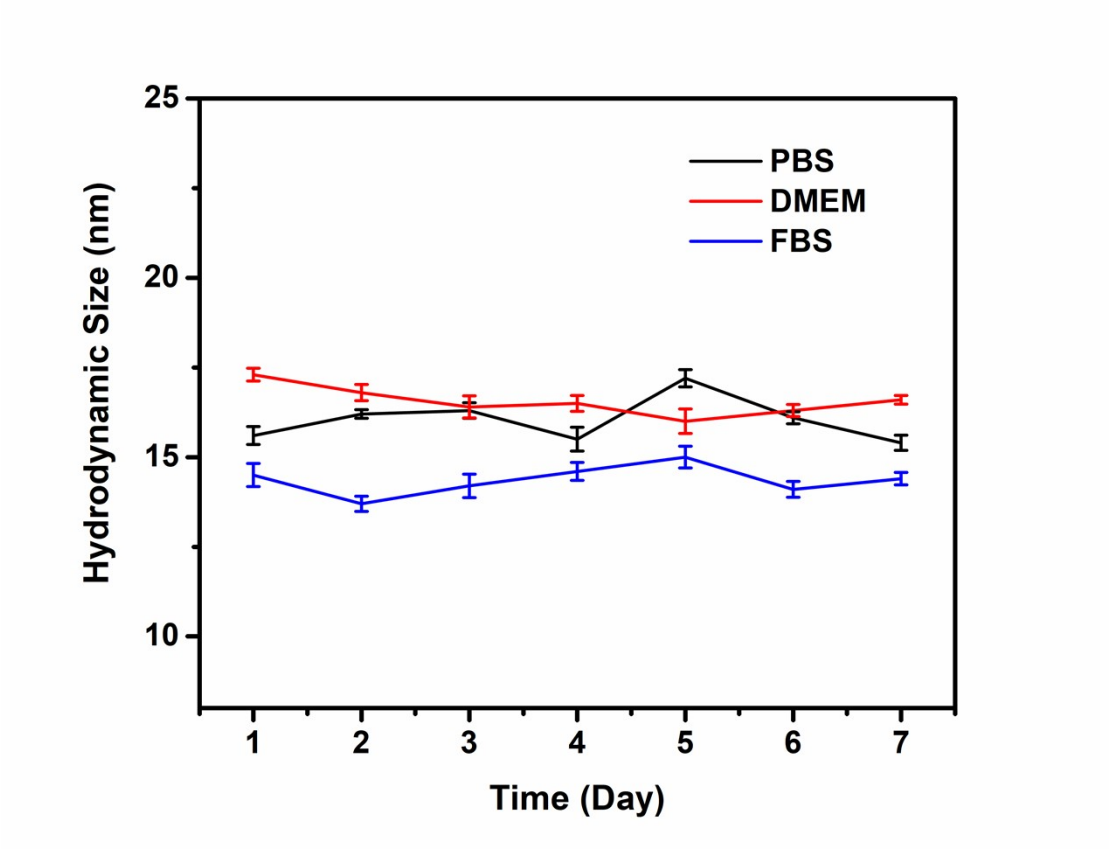

Figure S5. The size change of BSA@Gd_2O_3/IrO_2 NPs after incubation with PBS, serum, and culture medium for 7 days.

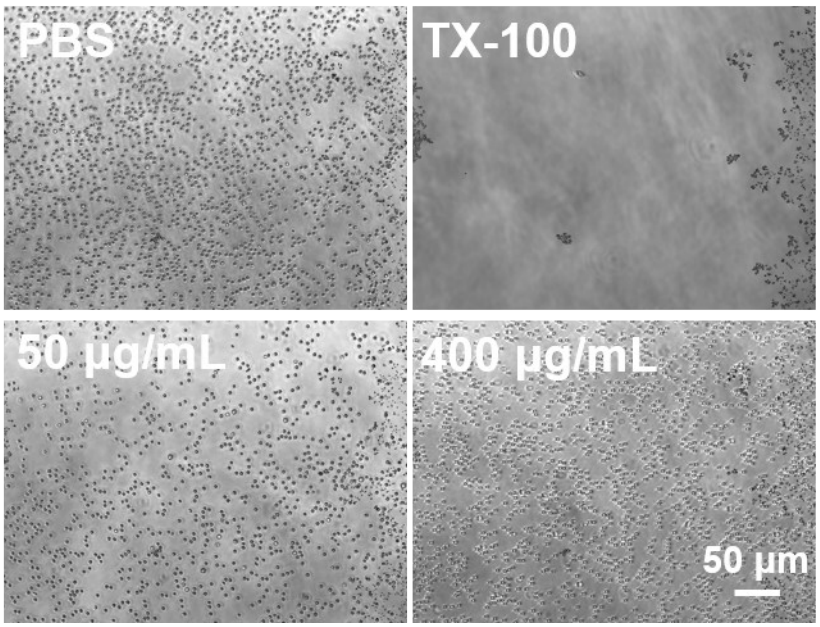

Figure S6. Morphology of mice red blood cells upon treatment with PBS, Triton X-100, and BSA@Gd_2O_3/IrO_2 NPs (50, 400 μg mL^{-1}) for 2 h.

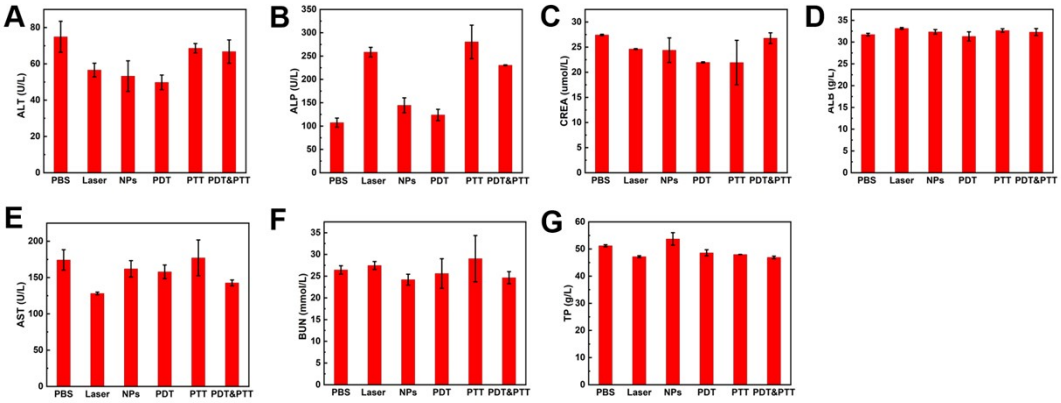

Figure S7. Blood biochemical tests on mice with various treatments.

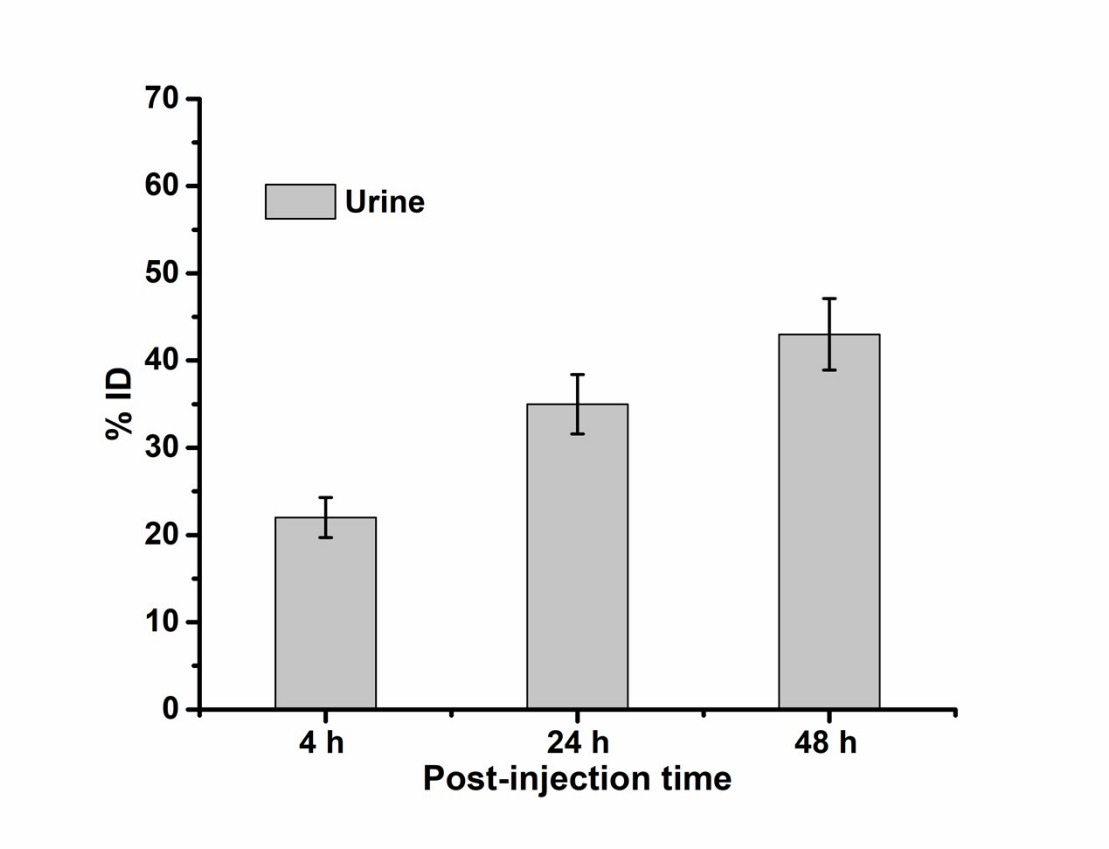

Figure S8. Cumulative clearance measurements of BSA@Gd_2O_3/IrO_2 NPs in urine at various post-injection time points to show the renal clearance.

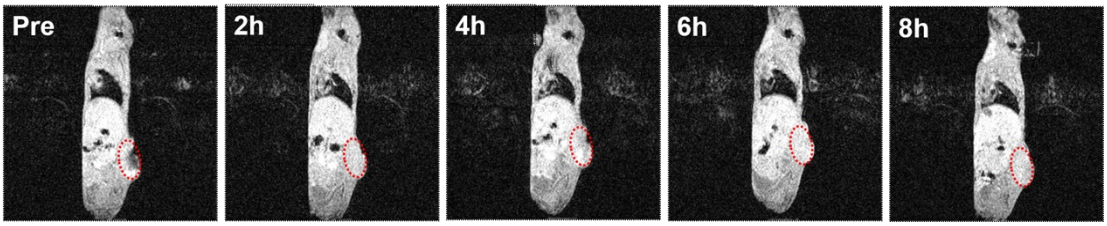

Figure S9. *In vivo* MR imaging of 4T1 tumor-bearing mice upon treatment with BSA@Gd_2O_3/IrO_2 NPs (Gd equivalent concentration: 1.5 mM).

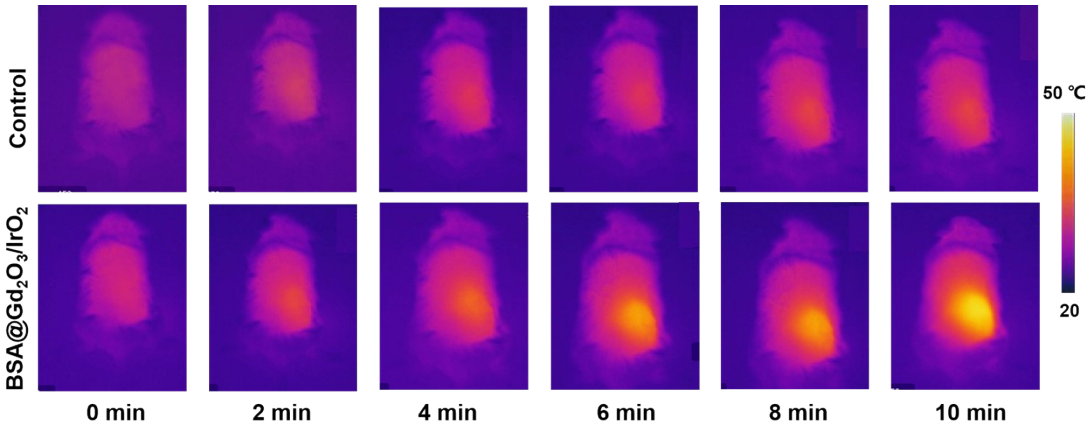

Figure S10. *In vivo* tumor temperature monitoring of the mouse injected with PBS and BSA@Gd_2O_3/IrO_2 NPs.

Reference

1. D. K. Roper, W. Ahn and M. Hoepfner, *Journal of Physical Chemistry C*, 2007, **111**, 3636-3641.